Electrochimica Acta 230 (2017) 454–460

Contents lists available at ScienceDirect

Electrochimica Acta

journal homepage: www.elsevier.com/locate/electacta

Research Paper

Effects of rest time after Li plating on safety behavior—ARC tests with commercial high-energy 18650 Li-ion cells

Thomas Waldmann*, Margret Wohlfahrt-Mehrens

ZSW – Zentrum für Sonnenenergie- und Wasserstoff-Forschung Baden-Württemberg, Helmholtzstrasse 8, D-89081 Ulm, Germany

ARTICLE INFO

Article history:
Received 13 October 2016
Received in revised form 6 February 2017
Accepted 7 February 2017
Available online 7 February 2017

Keywords:
Lithium-ion cells
Lithium plating
relaxation
thermal runaway
accelerated rate calorimetry (ARC)

ABSTRACT

During charging at low temperatures, metallic Lithium can be deposited on the surface of graphite anodes of Li-ion cells. This Li plating does not only lead to fast capacity fade, it can also impair the safety behavior. The present study observes the effect of rest periods between Li plating and subsequent accelerated rate calorimetry (ARC) tests. As an example, commercial 3.25 Ah 18650-type cells with graphite anodes and NCA cathodes are cycled at 0 °C to provoke Li plating. It is found that the rest period at 25 °C between Li plating and the ARC tests has a significant influence on the onset temperature of exothermic reactions (T_{SH}), the onset temperature of thermal runaway (T_{TR}), the maximum temperature, the self-heating rate, and on damage patterns of 18650 cells. The results are discussed in terms of chemical intercalation of Li plating into adjacent graphite particles during the rest period. The exponential increase of capacity recovery and T_{SH} as a function of time suggests a reaction of 1st order for the relaxation process.

1. Introduction

Today Li-ion technology is used for energy storage in a variety of applications such as smartphones, smartwatches, tablet/laptop computers, mp3 players, power tools, stationary energy storage, human spaceflight, unmanned aerial vehicles (UAV), light electric vehicles (LEV), as well as electric cars (EV, HEV, PHEV). During the whole life of a battery, the safety is most important.

Unfortunately, the life-time of state-of-the art Li-ion cells is limited by aging mechanisms on the material level [1–6]. One critical aging mechanism under investigation is Li plating on graphite anodes [5–20]. The reason for Li plating are negative anode potentials vs. Li/Li^+, which can be determined in full cells with an additional reference electrode [5,7,9,17,18]. During charging of a cell, the anode potential gets lower and the cathode potential increases. The difference between anode and cathode potential is the cell voltage [17,18].

The tendency of lower anode potentials is favored by low temperatures [5–7,17–19,21], high charging C-rates [6,9,18], and high SOC [7,9,18]. The combination of these parameters determines if Li plating happens or not [18].

An overview on possible processes (i-v) on the anode surface involving Li is shown in Fig. 1. During charging under Li plating conditions, there is a rivalry between intercalation of Li^+ ions from the electrolyte into graphite (ii) and deposition of metallic Li on the surface of the graphite anode (iv) [10,14,22]. This rivalry can be regarded as parallel reactions. During discharging with Li plating present on the graphite surface, metallic Li is stripped (iii) [14,21] and intercalated Li is de-intercalated (i). During a rest period, metallic Li can also chemically intercalated into adjacent graphite particles (v) [11,23].

The dendritic growth of metallic Li is often discussed as a main safety concern regarding Li plating [24–27]. The reason is that Li dendrites lead to internal short circuits between anode and cathode and could cause thermal runaway. We would like to stress that dendrite growth is not the only problem, since massive Li plating on anodes – which had not necessarily grown dendritically – leads to stronger exothermic reactions with electrolyte in differential scanning calorimetry (DSC) experiments [13].

On the cell level, a measure for cell safety is the onset temperature of exothermic reactions T_{SH} in accelerated rate calorimetry (ARC) tests [13,28–32]. In ARC tests, cells are heated step-by-step under quasi-adiabatic conditions until exothermic reactions are detected (heat-wait-seek experiment) [13,29,30,33]. In particular, a recent study on commercial cells with Li plating in our lab[13] showed

* Corresponding author at: Tel.:+ +49 0 731 9530 212; fax: +49 0 731 9530 666.
E-mail address: thomas.waldmann@zsw-bw.de (T. Waldmann).

http://dx.doi.org/10.1016/j.electacta.2017.02.036

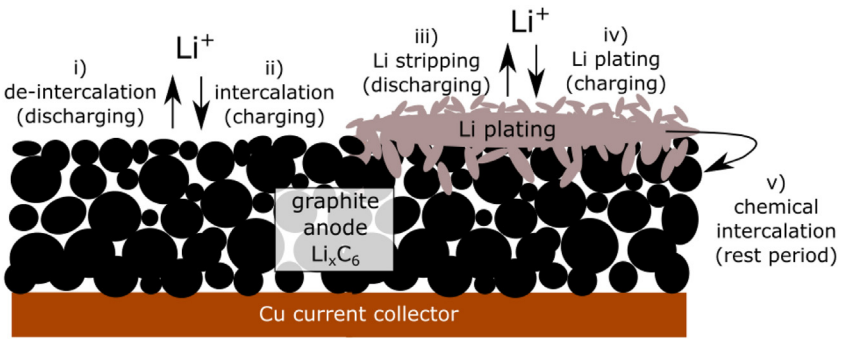

Fig. 1. Overview on possible processes on a graphite anode surface involving Li: Li intercalation into graphite (ii) and Li deposition on the anode surface (iv) during charging, Li de-intercalation from lithiated graphite (i) and stripping of deposited metallic Li (iii) during discharging. During a rest period, metallic Li can chemically intercalate into graphite if it is in direct contact (v).

(i) a stronger exothermic reaction of graphite anodes in DSC experiments,
(ii) a stronger degree of destruction after thermal runaway (ejection of jelly roll),
(iii) a low onset temperature in the range of 30–53 °C leading to thermal runaway under the quasi-adiabatic conditions in ARC tests.

One effect on safety behavior that has to best of our knowledge not been investigated so far is a rest period after Li plating. Mandeltort and Yates measured the intercalation kinetics of adsorbed Li submonolayers into graphite single crystals (HOPG) under ultra-high vacuum conditions [23]. Their measurements showed that Li moves from the graphite surface into the graphite with a comparably low activation barrier of 0.16 ± 0.02 eV [23]. Fan and Tan found by analysis of voltage curves that Li plating produced during charging at −20 °C diffuses into the graphite anode within 10 h at room temperature [8]. Dilation measurements by Bauer et al. showed a decrease of the thickness of pouch cells after charging at −5 °C [20]. Zinth et al. investigated the relaxation of lattice constants of commercial graphite/NMC cells with Li plating by neutron diffraction [11]. The authors found that during a rest period of 17–20 h, LiC_{12} is transformed into LiC_6 indicating the chemical intercalation of metallic Li into graphite [11].

Since Li in its metallic form is the cause for decreased safety behavior [13], it can be expected that chemical intercalation of Li plating into adjacent graphite and the results of thermal runaway tests are correlated. Since there is a dearth of knowledge on this is topic, this is investigated in the present study. Furthermore, damage patterns of the cells after thermal runaway are evaluated for cells with and without Li plating.

2. Experimental

All electrochemical tests were performed by a Basytec CTS system in combination with climate chambers (Vötsch). The high-energy 18650 cells under investigation include NCA cathodes, they have a specified minimum capacity of 3.25 Ah, a cell voltage range of 2.5–4.2 V, and a nominal voltage of 3.6 V. The cell weight with external tabs and without plastic shell is 46.0 g.

From previous investigations in our lab it is known that this cell type reaches ∼80% of the initial capacity after 18 cycles at 0 °C when charged and discharged at 0.5C (CC-CV charging to end-of charge voltage/cut-off current: 0.165A and CC discharging to end-of-discharge voltage) [9]. Therefore these conditions were used to provoke Li plating. The rest period between charging and discharging was 10s. Cycling started with the cell at 3.6 V and ended with a charged cell. Consequently, the ARC tests were performed with the cells charged to 4.2 V (CC-CV) at the cycling temperature of 0 °C and at 25 °C for the fresh cells.

The cells with Li plating were subject to ARC tests after rest periods of 1.5 h and 8d after cycling. For comparison, fresh cells were charged with a rate of 0.2C at 25 °C, which is known not to lead to Li plating for this cell type [9]. In order to exclude any effects of low cell temperature in combination with the ARC temperature control loop, additional fresh cells were cooled down to 0 °C for 2 h, before they were heated to 25 °C for 1.5 h similar to the cells with Li plating. These cells showed a very similar behavior to the fresh cells handled at 25 °C only and therefore effects of the cell

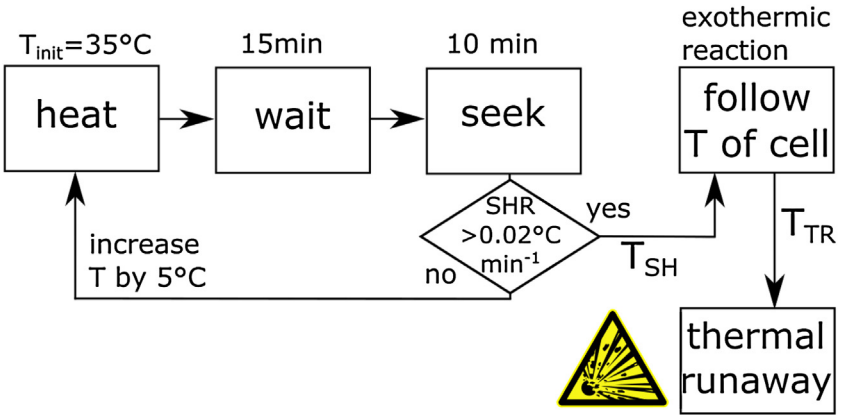

Fig. 2. Heat-wait-seek algorithm used to force the cells into thermal runaway.

temperature on the ARC results can be excluded. All ARC tests were reproduced at least with one additional cell operated under the same conditions.

The quasi-adiabatic tests were performed in an ARC-EV (Thermal Hazard Technology). The temperature of the 18650 cells was measured on the cell surface during the test. The self-heating rate (SHR) was calculated from the temperature and time data. ARC tests were performed in the heat-wait-seek mode, whereby the temperature was raised in steps of 5 °C followed by a wait period of 15 min and a seek period of 10 min. The cell temperature was followed if SHR >0.02 °C min^{-1} during the seek-period (see Fig. 2). All cells in this study were tested charged to 4.2 V.

The onset of self-heating T_{SH} was determined from the SHR data. When the threshold of 0.02 °C/min was exceeded for the first time, the corresponding temperature is T_{SH}. The onset of thermal runaway T_{TR} was determined from SHR vs. T plots (e.g. Fig. 6). Lines were fitted to data points before and after the change of the slope. The temperature at which the lines cross each other is T_{TR}.

Additionally, cells cycled 18 times at 0 °C were tested after different rest periods (1.5 h–32d) in the ARC. The "heat-wait-seek-repeat" algorithm (see Fig. 3), was used to create more data points with different rest time by re-using the same cells for subsequent measurements (result shown in Fig. 10). When T_{SH} was determined in an ARC run (threshold: SHR >0.02 °C min^{-1}), the test was stopped to prevent thermal runaway. After cool down of the calorimeter below 30 °C, the measurement was repeated with the same cell. This allowed acquiring additional data points with different rest times. In order to exclude effects of heating of the cells on the result of the experiment, it was repeated with 7 cells with different initial rest periods. The result was well reproducible as can be seen from Fig. 10.

For some additional tests shown in Fig. 10, a second cell type with a capacity of 1.5 Ah with graphite anodes and NMC/$LiMn_2O_4$ blend cathodes, a voltage range of 2.0–4.2 V, a nominal voltage of 3.6 V was used.

3. Results and discussion

3.1. Influence of rest period after Li plating on capacity recovery

Fig. 4a shows the discharge voltage curves during cycling at 0 °C. As found by Smart and Ratnakumar [21] and later by others [12,14,34,35], the voltage curves show a plateau which is due to stripping of metallic Li from the graphite anode. For the tested cell type, the occurrence of Li plating at 0 °C and a charging C-rate of 0.5C is also in accordance with our recent measurements of anode potentials vs. Li/Li$^+$ in reconstructed 3-electrode full cells [9]. Furthermore, we have recently shown that Li plating is indicated by a positive slope of the Arrhenius plot for cycling aging [5,9], i.e.

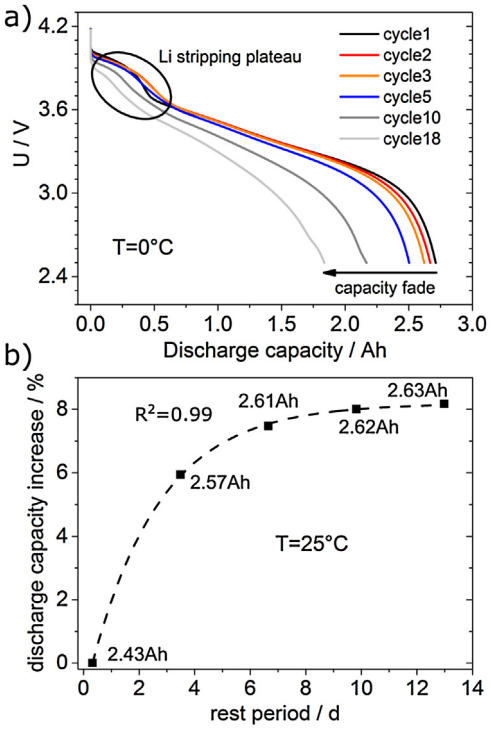

Fig. 4. a) Voltage curves during discharge for different cycles at an ambient temperature of 0 °C. b) Recovery of discharge capacity at an ambient temperature of 25 °C after Li plating had been created at 0 °C. The capacity increase is with respect to the capacity of the cells after aging. The dashed line corresponds to the fit with equation 1.

faster capacity fade with lower temperatures, which is also the case for the cell type tested here [9]. Therefore, Li plating on the graphite anodes of this cell type is also in full agreement with the cycling results at 0 °C [9].

Fig. 4b shows that the capacity is partly recovered during a rest period. In this experiment, the cell was firstly cycled at 0 °C to produce Li plating. Subsequently, the cell was heated to 25 °C and capacity tests were conducted every 72 h (charging: CC at 0.5C to 4.2 V, CV until I < C/20, discharging: CC at 0.5C until 2.5 V, again charging to 4.2 V). Fig. 4b shows that the capacity is increased as a function of rest time until it reaches saturation after ~13d. In particular, the cell capacity is increased by 8.1% after 311.6 h with respect to the first cycle at 25 °C.

In order to test the influence of the capacity tests, we performed additional tests in which the capacity was checked at 25 °C directly after the end of Li plating with a lower rate of C/10. After a rest period of 13d, the capacity had been recovered by 5.9%. We found a

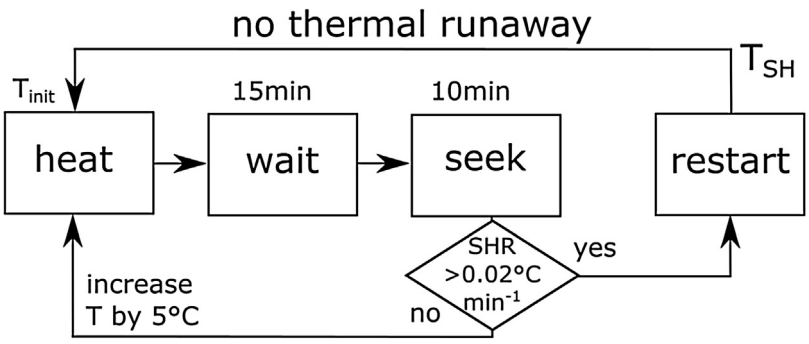

Fig. 3. Heat-wait-seek-repeat algorithm used to determine T_{SH} and prevent thermal runaway, allowing several measurements with the same cell.

similar value (5.0% after 12d) for capacity tests at 0.2C. Therefore, the capacity tests every 72 h are likely not to have a large influence on the capacity recovery. The capacity recovery is in agreement with results by others who found values of 6-9% if cells were continuously cycled at 25 °C after they had experienced Li plating at −22 °C. [19]

Furthermore, Fig. 4b shows that the time range for capacity recovery is in the order of two weeks. For 26650-type cells with graphite anodes and $LiFePO_4$ cathodes, a similar percentage of capacity recovery was reached after 300 cycles at 1C [19], corresponding to ~37.5d (in order to calculate the time from the number of cycles, we made the following assumption: 2 h CC-CV charging time and 1 h discharging time). The differences might arise from the different cell chemistry, cell design, and the fact the cells were cycled continuously in one case and every 72 h on the other case. Nevertheless, the time range is in a similar order of magnitude for both studies.

For a more quantitative evaluation of the capacity recovery, the data points were fit to the exponential function

$$y = a + b \cdot \exp(c \cdot t) \quad (1)$$

where a = 8.17802, b = −9.32066, and c = −0.40339 are constants, y is the capacity and t is the rest period. As can be seen from the high R^2-value of 0.99, the capacity recovery data are in very good agreement with Eq. (1).

The reason is most likely the reversibility of Li plating due to chemical intercalation of the metallic Li into the adjacent graphite particles. The observed exponential increase of the capacity recovery gives hints on the reaction order for intercalation of Li plating into graphite. Since similar exponential functions are observed in the ARC tests, this is discussed below.

The data presented in this section provide a sound basis for the presence of Li plating, Li stripping, and chemical intercalation of plated Li in the commercial 18650-type cells tested in this study. Since rest time after Li plating has most likely a significant effect on the reduction of metallic Li, the effect of rest time on the thermal runaway behavior was tested in the following section.

3.2. Influence of rest period after Li plating on thermal runaway in ARC tests

Fig. 5a shows the temperature profiles during ARC tests including the thermal runaway of the tested commercial 18650 cells for i) fresh cells without Li plating, ii) for cells with Li plating (after 1.5 h rest period), and iii) for cells with Li plating (after 8d rest period). It can be seen from Fig. 5a that both, time until thermal runaway and maximum temperature of thermal runaway are reproducible for each case.

We note that the fresh cells show the highest temperatures during thermal runaway. Fig. 5b shows a correlation between the discharge capacity and the maximum temperature during thermal runaway. It can be seen from the R^2-value of 0.94 that the data points are in good agreement with a linear fit. The reason for this correlation is most likely that the higher electrochemical energy content of cells with more capacity which is transformed into more heat and therefore leading to higher temperatures during thermal runaway. Other authors reported a similar trend for other types of 18650 cells charged to different SOCs [31,32]. Furthermore, the values of the maximum temperatures during thermal runaway reported by Yayathi et al. for 100% SOC (742.6 °C–786.4 °C) [31] are in a similar range like ours for the fresh cells.

Furthermore, Fig. 5a shows that the fresh cells without Li plating needs the longest time to reach the maximum temperature of thermal runaway (~1950 min). Interestingly, all tested cells with Li plating show significantly shorter times to reach the thermal

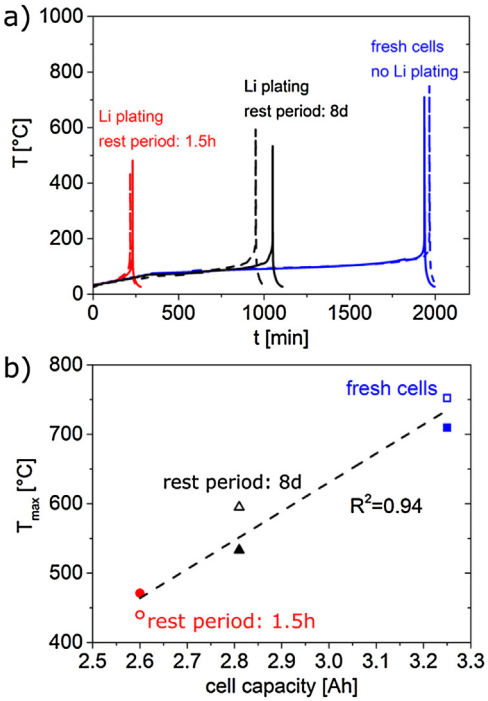

Fig. 5. a) Temperature curves of thermal runaway during ARC tests of fresh cells without Li plating (blue), cells with Li plating and a rest period of 1.5 h (red), and cells with Li plating and a rest period of 8d (black). Solid and dashed lines show reproductions of data with a second cell, respectively. b) Correlation of discharge capacity and maximum temperature during thermal runaway in ARC tests. Solid and open symbol show tests reproduced with a second cell, respectively. The dashed line corresponds to a linear fit. (For interpretation of the references to colour in this figure legend, the reader is referred to the web version of this article.)

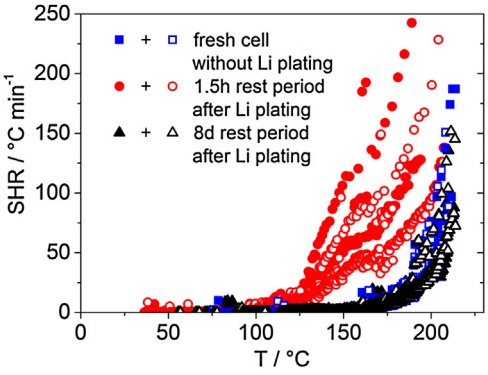

Fig. 6. Comparison of ARC tests with fresh cells (blue squares) and cells Li plating after a rest period of 1.5 h (red circles) and after 8d (black triangles). Filled and open symbols represent reproduction experiments (For interpretation of the references to colour in this figure legend, the reader is referred to the web version of this article.)

runaway and the maximum temperatures: For rest times of 1.5 h and 8d after Li plating, the maximum temperatures were reached after only ~225 min and ~1000 min, respectively.

Fig. 6 shows a plot of the SHR vs. temperature. The blue squares in Fig. 6 correspond to the fresh cells without Li plating. T_{SH} of these cells is observed at 75.6 °C, which is comparable with results from other cell types [13,33]. In our ARC tests on fresh cells, thermal runaway starts at 177.3 °C. This is also in the range reported for other cells [13,33].

For the fresh cells, we observed no ejection of the jelly roll after thermal runaway (see Fig. 7a). However, a significant amount of material had been ejected from the cell, as can be seen from the

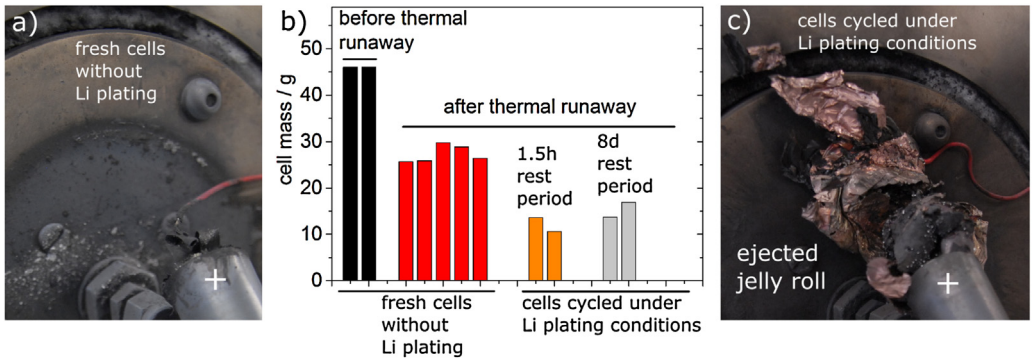

Fig. 7. a) No ejection of jelly roll from fresh cells without Li plating (typical image near the positive connector of the 18650 cell). b) Cell masses of fresh and aged 18650 cells before and after thermal runaway in ARC tests. c) Ejection of jelly roll from 18650 cells with Li plating (typical image near the positive connector of the cell). Please note that the jelly roll was ejected for all cells with Li plating, independently from the rest period.

reduced cell mass compared to the fresh cell (see Fig. 7b). Ejection of cell components was also reported for other cells during thermal runaway not induced by ARC by Finegan et al. [36]. Golubkov et al. found that the mass loss after thermal runaway of discharged cells is in a similar range like the mass of electrolyte in the cells, suggesting evaporation/combustion of the electrolyte [32]. In contrast, cells at 100% SOC showed a higher mass loss [31,32], which is in a similar range like in our tests with fresh cells and is related to ejection of additional material from the cell.

We note that the stronger damage pattern for the cells with Li plating (Fig. 7c) is not in line with the trend of the maximum temperature during thermal runaway (Fig. 5b). The reason it that the damage pattern is not only connected to the energy content, but also to other factors like the amount of gas formed during thermal runaway.

The red circles in Fig. 6 show the ARC result of the cells with a rest period of 1.5 h after Li plating. In strong contrast to the fresh cells, T_{SH} is observed already at 36.4 °C. T_{TR} is shifted to the lower temperature of 123.0 °C (130.4 °C for a second cell). Consequently, the SHR is significantly higher already at lower temperatures for the cells with Li plating after a rest period of 1.5 h. This is in agreement with our previous ARC results on 18650 cells with NMC/LMO blend cathodes and graphite anodes with Li plating [13]. The reason are stronger exothermic reactions of graphite anodes with Li plating as determined by DSC experiments [13]. We stress that in ARC experiments, the reason for the observed decrease of safety are not Li dendrites, although they are mostly mentioned in literature in combination with Li plating.

Golubkov et al. overcharged 18650 cells with NCA cathode to 143% SOC and found a similar trend of decreasing T_{SH} [32]. The reason is most likely that overcharging is also related with Li plating, since during charging the anode potential gets lower and is likely to get negative [5,7,9,17,18]. It has to be noted here that overcharging in their case has most likely also increased the cathode potential. It has to be further noted that T_{SH} was decreased by overcharging in the study by Golubkov et al., [32] but not to such low values as in our tests. This might be due to a higher amount of irreversible Li plating in our study produced by continuous cycling at low temperature.

In strong contrast to the fresh cells, the cells with Li plating and a rest time of 1.5 h were strongly decomposed during thermal runaway. As can be seen from Fig. 7c, the jelly roll was reproducibly mostly ejected from the cell housing. This is also reflected in the cell mass (Fig. 7b), which is about the half of that for the fresh cells after thermal runaway. Ejection of the jelly roll is in agreement with our earlier thermal runaway study with other types of 18650 cells with Li plating [13]. This violent decomposition of the cell with Li plating is connected to the low flash points of the typical carbonate electrolytes [37] in combination with the reactivity of metallic Li, especially when it gets liquid at 180.5 °C. It is noted that in all-solid-state cells with Li metal as anode material this might be less problematic due to the absence of flammable electrolyte.

The black triangles in Fig. 6 correspond to the ARC result of the cells with a rest period of 8d after Li plating. T_{SH}, T_{TR}, as well as the SHR curve shape are similar to the fresh cell. Corresponding to these values, the safety behavior has recovered during the rest period of 8d at 25 °C after Li plating.

However, as Fig. 7c shows, the jelly roll was also ejected reproducibly for the cells with a rest period of 8d after Li plating. This can also be seen from the cell mass after thermal runaway, which is similar to the cells with a rest time of 1.5 h. Therefore, the damage pattern has not recovered by the rest period. The reason is most likely contact loss of metallic Li and the anode during the rest period. Subsequently, a passivating film is formed on the Li surface preventing further reaction. Therefore, metallic Li is likely to be present in an enclosed form. However, during thermal runaway, this enclosed metallic Li gets liquid and leads to a stronger decomposition reaction of the cell. Therefore, although Li plating is partly reduced by chemical intercalation, it is still a latent risk for the cell safety.

3.3. Arrhenius analysis of ARC results

Fig. 8 shows an Arrhenius analysis of the ARC results. In this plot ln(SHR) is plotted on the y-axis, whereas the $1/k_BT$ is on the x-axis

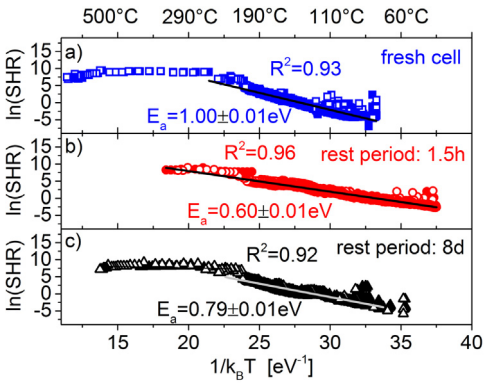

Fig. 8. Arrhenius plots of SHR during thermal runaway in ARC tests. The fits were made with two separately reproduced cells (filled and open symbols), respectively.

(k_B: Boltzmann constant, T: absolute temperature, A: pre-exponential factor). According to[38]

$$\ln(SHR) = \ln(A) - E_a\left(\frac{1}{k_B T}\right) \quad (2)$$

the data points of associated reproduced cells in the Arrhenius plots were fit with lines, whose slopes $-E_a$ correspond to activation barriers.

Fig. 8a shows two temperature regimes for the ARC tests of fresh cells. From ~75 °C to ~260 °C, the data can be fitted with a line, indicating Arrhenius-like behavior ($R^2 = 0.93$, ln (A) = 27.77 ± 0.22). In the lower temperature range, the slope of the Arrhenius plot yields an activation barrier of 1.00 ± 0.01 eV, which is comparable to our earlier results on fresh cells of another type [13]. Above ~260 °C, the slope gets flat making an interpretation difficult.

Fig. 8b shows only one temperature regime for the ARC tests of the cells with a rest period of 1.5 h after Li plating. The slope of a linear fit to the data points yields an activation barrier of 0.60 ± 0.01 eV ($R^2 = 0.96$, ln(A) = 20.00 ± 0.07), which is significantly lower compared to the fresh cell. The value of the activation barrier is very similar than found in our earlier study on other cell types with Li plating [13]. This indicates a similar decomposition mechanism for both cell types with Li plating. Furthermore, it can be concluded that the decomposition mechanism for cells with Li plating and a rest time of 1.5 h is significantly different from that of the fresh cell, as indicated by either one or two temperature regimes as well as the different activation barriers.

Fig. 8c shows the Arrhenius plot for the cell with a rest period of 8d after Li plating. In similarity to the fresh cell, two temperature regimes are observed. However, the activation barrier of 0.79 ± 0.01 eV ($R^2 = 0.92$, ln(A) = 22.66 ± 0.19) is between that of the fresh cell and the cell with Li plating and a rest period of 1.5 h.

The reason for the observed partly recovery of safety behavior is most likely due to the chemical intercalation of a part of the plated Li into adjacent graphite particles during the rest period. In order to shed light on this phenomenon, the effect of the rest period on T_{SH} in cells with Li plating is investigated in the next section.

3.4. Reaction kinetics of relaxation process during the rest period

Fig. 9 shows the decrease of the SHR during the seek-period of the ARC test starting at 35 °C as a function of rest time after Li plating. The data points in Fig. 9 can be fit to an exponential function (eq. 1 with y = SHR, $R^2 = 0.97$). The data shown in Fig. 9 are on a similar time scale as reported for chemical intercalation of Li

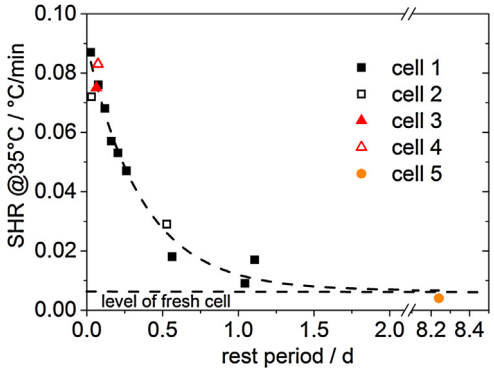

Fig. 9. Decrease of self-heating rate as a function of rest time after Li plating. The data points were recorded during the seek-period with the ARC set to 35 °C. The dashed line corresponds to the fit with Eq. (1).

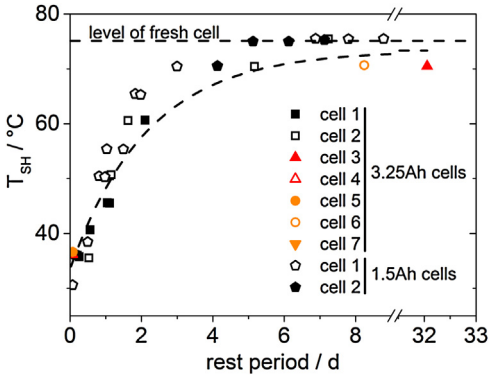

Fig. 10. Increase of onset temperature in ARC tests as a function of rest time after Li plating for the 3.25 Ah cells after 18 cycles at 0 °C. Please note that the pentagonal data points are from another cell type (1.5 Ah cells) which shows a similar behavior after 50 cycles at 0 °C. The dashed line corresponds to the fit with Eq. (1).

plating into graphite reported by Zinth et al. using neutron diffraction [11].

As the SHR with the ARC set to 35 °C decreases with time, consequently T_{SH} is shifted to higher temperatures. This is shown in Fig. 10, where T_{SH} is plotted as a function of rest time after Li plating. Similar to Figs. 4 b and Fig. 9, the data points in Fig. 10 can be fit to an exponential function (eq. 1 with y = T_{SH}, $R^2 = 0.95$, a = 73.33184, b = −39.79550, c = −0.46242).

We note that the time scale of the data in Fig. 10 is longer compared to that in Fig. 9. The reason is that in Fig. 10, additional data for higher temperature is shown. On the other hand, the data in Fig. 10 is on a very similar time scale as the capacity recovery during the rest (Fig. 4b). Therefore, it is likely that both, recovery of capacity and T_{SH} are linked to similar relaxation processes.

Under the reasonable assumption that the self-heating of the cell is mainly caused by the reaction of plated Li with electrolyte, the decay of the SHR is likely to reflect the amount of Li plating in the cell. Due to their exponential decays, the observed data point towards a (pseudo) 1st order reaction [38].

An exponential decay can also be estimated from the changes of integral intensities for LiC_6 and LiC_{12} during the rest time after Li plating by Zinth et al. [11]. However, it has to be discussed that the authors found a relaxation of these values in a time range of 20 h and at the lower temperature of −20 °C. For the temperature of 25 °C in our experiments, it can be expected that the reaction is accelerated. Fan and Tan reported that plated Li diffuses into graphite at 25 °C within 10 h, [8] which is also a shorter time scale than in our case. However, Figs. 4 b and Fig. 10 both show relaxations in the range of 1 week. It has to be taken into account that the relaxation time is likely to be influenced by a variety of factors including, the morphology of Li plating, the anode material, the particle size distribution, porosity/tortuosity of the anode, the electrolyte, and the pressure inside the cell. Therefore, it is difficult to directly compare the time scale of our results with literature.

In order to exclude that the cell type investigated in this study (3.25 Ah 18650 cells) shows a specific relaxation behavior, we performed a limited test series with another cell type (1.5 Ah 18650 cells). This second cell type was cycled 50 times at 0 °C, similar to our previous study with the same cell type [5]. From our previous studies, we know that these conditions lead to Li plating in this cell type [5,13]. As can clearly be seen from the pentagonal data points in Fig. 10, this second cell type shows a similar relaxation behavior of T_{SH} as a function of rest time after Li plating. Therefore, this observation is not limited to the 3.25 Ah cells investigated mainly in the present study.

4. Conclusions

In the present paper, it was confirmed that Li plating on graphite anodes can have a significant effect on the safety behavior of Li-ion cells under the quasi-adiabatic conditions of ARC tests. We stress that in this case, the thermal runaway is not induced by Li dendrites but most likely due to the stronger exothermic reactions of metallic Li.

In order to account for the worst case scenario in safety tests, we suggest that cells could be tested not only in the fresh state, but also directly after cycling under Li plating conditions. The rest time after Li plating has a significant influence on the result of ARC tests and has therefore to be considered to get accurate measurements with cells with Li plating on graphite anodes.

In particular, for commercial 18650-type cells with graphite anodes and NCA cathodes and a capacity of 3.25Ah, we reproducibly found in ARC tests conducted 1.5 h after Li plating at 0 °C:

1) The time in ARC tests until thermal runaway is reached is significantly reduced compared to fresh cells.
2) The onset of self-heating is shifted to significantly lower temperatures (~35 °C for 1.5 h rest time).
3) A more violent decomposition of the cells with Li plating is found in ARC tests. The damage pattern reproducibly included ejection of the jelly roll from the cell housing. This damage pattern is not observed for fresh cells without Li plating.

In contrast, fresh cells show higher maximum temperatures during thermal runaway in ARC tests. The reason is most likely their higher electrochemical energy content.

Chemical intercalation of metallic Li into adjacent graphite particles during rest time can reduce Li plating. Therefore, a rest period of 8d at in the charged state at 25 °C after Li plating leads to a partial recovery of the cell:

1) A part of the cell capacity is recovered during the rest time.
2) The time until thermal runaway is reached in ARC tests is between that of cells with Li plating after a rest period of 1.5 h and fresh cells.
3) The onset of self-heating is shifted to higher temperatures and is similar to the fresh cells.
4) The onset of thermal runway is shifted to higher temperatures, similar to the fresh cells.
5) The damage pattern is similar for the cells with a rest period of 1.5 h after Li plating (ejection of jelly roll from cell housing) and is therefore not recovered.

The fact that the safety level of the fresh cell is not reached for all cases is an indication for irreversible Li plating still being inside the cell. This enclosed form of metallic Li, most likely covered by a passivating film is a latent safety risk. As a consequence, Li plating has to be avoided in Li-ion cells by taking action on the level of operating parameters as well as on the material level for the next cell generations.

Since the capacity recovery, the SHR at 35 °C and the onset temperature as a function of rest time are exponential functions, it is likely that the relaxation process of chemical intercalation of Li plating into graphite is a (pseudo) 1st order reaction.

The current results strongly suggest that the safety of Li-ion cells is not simply a function of capacity loss. The pathway how the capacity is lost – i.e. by which aging mechanisms – has to be considered. Further studies in this direction are ongoing in our lab.

Acknowledgement

The research leading to these results has been performed within the MAT4BAT project (http://mat4bat.eu/) and received funding from the European Community's Seventh Framework Programme (FP7/2007-2013) under grant agreement n°608931. We thank J. Kramarczyk (ZSW) for help with a part of the measurements with the 1.5 Ah cells in Fig. 10 as well as P. Axmann (ZSW) and the Thermal Hazard Technology (THT) team for helpful discussions.

References

[1] M. Wohlfahrt-Mehrens, C. Vogler, J. Garche, J. Power Sources 127 (2004) 58–64.
[2] M. Broussely, et al., J. Power Sources 146 (2005) 90–96.
[3] J. Vetter, et al., J. Power Sources 147 (2005) 269–281.
[4] M. Ecker, et al., J. Power Sources 248 (2014) 839–851.
[5] T. Waldmann, M. Wilka, M. Kasper, M. Fleischhammer, M. Wohlfahrt-Mehrens, J. Power Sources 262 (2014) 129–135.
[6] J.C. Burns, D.A. Stevens, J.R. Dahn, J. Electrochem. Soc. 162 (2015) A959–A964.
[7] H.-P. Lin, et al., Electrochem. Solid-State Lett. 4 (2001) A71.
[8] J. Fan, S. Tan, J. Electrochem. Soc. 153 (2006) A1081.
[9] T. Waldmann, M. Kasper, M. Wohlfahrt-Mehrens, Electrochimica Acta 178 (2015) 525–532.
[10] N. Ghanbari, T. Waldmann, M. Kasper, P. Axmann, M. Wohlfahrt-Mehrens, ECS Electrochem. Lett. 4 (2015) A100–A102.
[11] V. Zinth, et al., J. Power Sources 271 (2014) 152–159.
[12] M. Petzl, M.A. Danzer, J. Power Sources 254 (2014) 80–87.
[13] M. Fleischhammer, T. Waldmann, G. Bisle, B.-I. Hogg, M. Wohlfahrt-Mehrens, J. Power Sources 274 (2015) 432–439.
[14] S. Hein, A. Latz, Electrochimica Acta 201 (2016) 354–365.
[15] S. Tippmann, D. Walper, L. Balboa, B. Spier, W.G. Bessler, J. Power Sources 252 (2014) 305–316.
[16] B. Bitzer, A. Gruhle, J. Power Sources 262 (2014) 297–302.
[17] B.-I. Hogg, M. Wohlfahrt-Mehrens, Meeting Abstracts, The Electrochemical Society, 2015, pp. 343.
[18] T. Waldmann, et al., J. Electrochem. Soc. 163 (2016) A1232–A1238.
[19] M. Petzl, M. Kasper, M.A. Danzer, J. Power Sources 275 (2015) 799–807.
[20] M. Bauer, M. Wachtler, H. Stöwe, J.V. Persson, M.A. Danzer, J. Power Sources 317 (2016) 93–102.
[21] M.C. Smart, B.V. Ratnakumar, J. Electrochem. Soc. 158 (2011) A379.
[22] N. Ghanbari, T. Waldmann, M. Kasper, P. Axmann, M. Wohlfahrt-Mehrens, J. Phys. Chem. C 120 (2016) 22225–22234.
[23] L. Mandeltort, J.T. Yates, J. Phys. Chem. C 116 (2012) 24962–24967.
[24] S.J. Harris, A. Timmons, D.R. Baker, C. Monroe, Chem. Phys. Lett. 485 (2010) 265–274.
[25] C.T. Love, O.A. Baturina, K.E. Swider-Lyons, ECS Electrochem. Lett. 4 (2014) A24–A27.
[26] J. Steiger, D. Kramer, R. Mönig, J. Power Sources 261 (2014) 112–119.
[27] M. Jäckle, A. Groß, J. Chem. Phys. 141 (2014) 174710.
[28] M.N. Richard, J.R. Dahn, J. Electrochem. Soc. 146 (1999) 2068.
[29] J.S. Gnanaraj, et al., J. Power Sources 119–121 (2003) 794–798.
[30] H. Maleki, G. Deng, A. Anani, Howard, J. Electrochem. Soc. 146 (1999) 3224.
[31] S. Yayathi, W. Walker, D. Doughty, H. Ardebili, J. Power Sources 329 (2016) 197–206.
[32] A.W. Golubkov, et al., RSC Adv. 5 (2015) 57171–57186.
[33] E. Roth, D. Doughty, J. Power Sources 128 (2004) 308–318.
[34] S. Hein, A. Latz, ECS Trans. 69 (2015) 3–5.
[35] S. Schindler, M. Bauer, M. Petzl, M.A. Danzer, J. Power Sources 304 (2016) 170–180.
[36] D.P. Finegan, et al., Nat. Commun. 6 (2015) 6924.
[37] S. Hess, M. Wohlfahrt-Mehrens, M. Wachtler, J. Electrochem. Soc. 162 (2015) A3084–A3097.
[38] P.W. Atkins, Physical Chemistry, Oxford University Press, Oxford: New York, 1990.